

This is a repository copy of *An optically multiplexed single-shot time-resolved probe of laser–plasma dynamics*.

White Rose Research Online URL for this paper:

<https://eprints.whiterose.ac.uk/142368/>

Version: Published Version

---

**Article:**

Davidson, Zoe, Gonzalez-Izquierdo, Bruno, Higginson, Adam et al. (7 more authors)  
(2019) An optically multiplexed single-shot time-resolved probe of laser–plasma dynamics.  
Optics Express. pp. 4416-4423. ISSN 1094-4087

<https://doi.org/10.1364/OE.27.004416>

---

**Reuse**

This article is distributed under the terms of the Creative Commons Attribution (CC BY) licence. This licence allows you to distribute, remix, tweak, and build upon the work, even commercially, as long as you credit the authors for the original work. More information and the full terms of the licence here:

<https://creativecommons.org/licenses/>

**Takedown**

If you consider content in White Rose Research Online to be in breach of UK law, please notify us by emailing [eprints@whiterose.ac.uk](mailto:eprints@whiterose.ac.uk) including the URL of the record and the reason for the withdrawal request.



# An optically multiplexed single-shot time-resolved probe of laser–plasma dynamics

Z. E. DAVIDSON,<sup>1</sup> B. GONZALEZ-IZQUIERDO,<sup>1</sup> A. HIGGINSON,<sup>1</sup> K. L. LANCASTER,<sup>2</sup> S. D. R. WILLIAMSON,<sup>1</sup> M. KING,<sup>1</sup> D. FARLEY,<sup>2</sup> D. NEELY,<sup>1,3</sup> P. MCKENNA,<sup>1</sup> AND R. J. GRAY<sup>1,\*</sup>

<sup>1</sup>*Department of Physics, SUPA, University of Strathclyde, Glasgow, UK*

<sup>2</sup>*Department of Physics, University of York, York, UK*

<sup>3</sup>*Central Laser Facility, STFC Rutherford Appleton Laboratory, Didcot, Oxfordshire, UK*

\**ross.gray@strath.ac.uk*

**Abstract:** We introduce a new approach to temporally resolve ultrafast micron-scale processes via the use of a multi-channel optical probe. We demonstrate that this technique enables highly precise time-resolved, two-dimensional spatial imaging of intense laser pulse propagation dynamics, plasma formation and laser beam filamentation within a single pulse over four distinct time frames. The design, development and optimization of the optical probe system is presented, as are representative experimental results from the first implementation of the multi-channel probe with a high-power laser pulse interaction with a helium gas jet target.

Published by The Optical Society under the terms of the [Creative Commons Attribution 4.0 License](#). Further distribution of this work must maintain attribution to the author(s) and the published article's title, journal citation, and DOI.

## 1. Introduction

Laser-plasma interactions attract significant research interest in part because they offer a route to accessing exotic states of matter, including fusion plasmas [1], and as a compact source of radiation [2]. It has been a central aim in these topics to experimentally measure the temporal and spatial evolution of the underpinning dynamics which drive the interaction.

The complex dynamics of these interactions evolve rapidly on timescales less than the laser pulse (femto- to pico-seconds) and are highly sensitive to initial plasma conditions and shot-to-shot variations in the laser pulse parameters [3]. There have been a number of recent results that highlight the sensitivity of the source properties to changes in the laser and plasma parameters within a narrow range [4–6]. Although some of these dynamics can be elucidated in numerical simulations, due to limitations in the physical processes that can be included in codes and the use of idealized input parameters, measurements in the laboratory give the most comprehensive insights. There presently exists a growing need for the development of experimental techniques which enable detailed and controlled investigation with high spatial and temporal resolution in order to investigate complex evolving laser–plasma dynamics such as self-focusing [7] or the propagation of higher-order modes (such as Laguerre-Gaussian beams) in plasma [8]. Progress in this area will open up a new dimension of experimental measurement and provide additional capability to quantify key factors which limit the control of laser–plasma-driven radiation sources.

To date a number of experimental techniques have been developed which seek to address this challenge such as proton probing [9, 10] and the use of a streak camera [11, 12]. Both of these, however, have limitations, in temporal resolution and versatility [13, 14], and spatial dimensionality [15], respectively. Optical probing using a chirped laser pulse [16, 17] has also recently been investigated to provide temporal resolution however, with the dependence on pulse bandwidth, this approach does not work well for picosecond scale systems and lacks arbitrary control over the temporal resolution. Complementary to all of these, single pulse optical probing is often used over multiple consecutive shots at varied probe timings in order to construct a temporal series [18]. This method is inherently susceptible to changes in the interaction dynamics

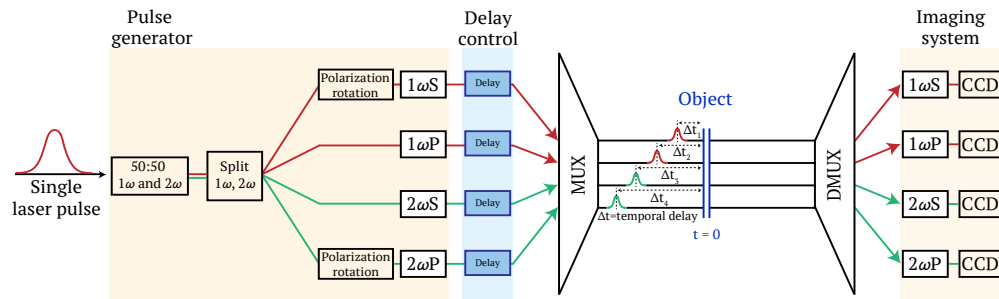


Fig. 1. Process flow diagram of multiplexed optical probe concept. A single ultrashort laser pulse is divided into four separate laser pulses which are uniquely encoded by frequency and polarization. The four pulses are independently delayed in time and then spatially multiplexed (MUX) to propagate co-linearly in order to optically probe a given point in space and time. The inverse process (DMUX) is then applied to spatially separate and form an image for each of the channels. This enable 2D spatial and picosecond temporal resolution over multiple frames with a single laser pulse.

due to shot-to-shot variations in the laser and plasma conditions [19–22], including changes in the laser spatial profile, energy and spectrum. This issue can be compounded by the fact that many large laser systems have low shot rates and low output stability, and therefore poor statistics with which to minimize the impact of shot-to-shot fluctuation on measurements [19]. This is a critical limitation highlighted as motivation for the development of alternative temporal measurement techniques such as time-sequence imaging by two-color probe [23].

In this article, we present the design and the first measurements of a temporally resolved laser–plasma interaction tracking the propagation of a single laser pulse using a novel multi-channel probe. We demonstrate that this optical probe system enables picosecond-scale temporal resolution and two-dimensional spatial resolution of a single interaction. With these measurements we demonstrate that small variations in initial conditions strongly influence the subsequent interaction properties which consequently inhibits the reliability of optical probe measurements when obtained across repeated shots. This paper details the concept, design of the optical system and the first tests of the system on a high power laser–plasma experiment. Additionally, we envisage the multi-channel probe concept to potentially enhance existing approaches to temporally resolve ultra-fast phenomena across other fields of scientific research that are also inherently susceptible to stochastic phenomena [19], such as in pump-probe microscopy [24] and irreversible reaction dynamics [25].

## 2. System design

The fundamental principle of this new approach derives originally from the established wavelength and polarization division multiplexing techniques which have been used widely, primarily, in telecommunications for decades [26]. We now adapt this concept and implement a design which is appropriate for a pump-probe arrangement in a high power laser–plasma interaction environment. A process flow diagram of the optical probe system is shown in Fig. 1. The multi-channel optical probe system consists of one input channel and four temporally staggered and encoded output channels which enables four separate interferograms to be taken of an identical spatial location, with independent timing control. The multi-channel probe consists of four main parts: the pulse generator, where four individual pulses are generated from an initial seed pulse, encoded by wavelength and polarization and then appropriately delayed in time; the multiplexer where the separate pulses are made co-linear again; the demultiplexer which spatially separates the four pulses into individual imaging or interferometry and lastly, the imaging system

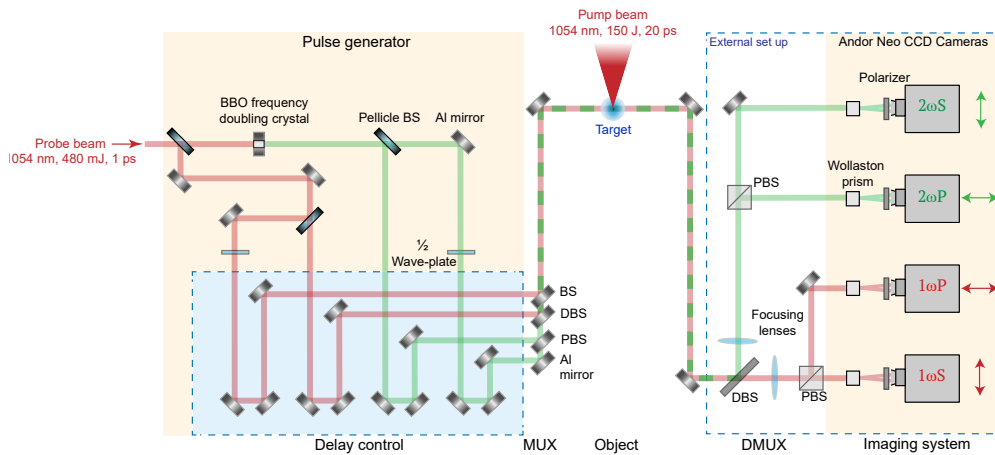


Fig. 2. Schematic of the experimental set up within the vacuum chamber where a high power pump laser pulse is focused into a gas target and a low-intensity probe pulse is passed through the internal multi-channel system and the demultiplex arrangement external to the chamber. The diagram details the optical system used in the multi-channel probe to generate the four uniquely encoded laser pulses, delay them in time, spatially multiplex and then demultiplex after the interaction point (object) to image the individual channels.

consisting of focusing lenses and CCD cameras.

A detailed technical schematic of the development from concept to the optical system design for use on a high power laser experiment is shown in Fig. 2. By splitting the initial P-polarized pulse in two, one output can be frequency doubled by passing it through a  $\beta$ -Barium Borate (BBO) crystal of 50% conversion efficiency. This generates  $1\omega$  (1054 nm) and  $2\omega$  (527 nm) channels which can both be divided again by a beamsplitter (BS), after which one of each harmonic is passed through a half wave-plate to give a  $90^\circ$  polarization rotation, to produce  $1\omega S$  and  $2\omega S$ . The final result is four laser pulses (henceforth referred to as  $1\omega S$ ,  $1\omega P$ ,  $2\omega S$  and  $2\omega P$ ) with uniquely distinguishable combinations of wavelength and polarization. To enable independent timing control of each of the laser pulses a time delay slide is included along each beam path. The individual delay stages facilitate both fine and coarse control of the intervals between imaging, providing flexibility to observe developments at arbitrary timesteps over a few picoseconds and at later stages of the remnants of the interaction with larger steps of hundreds of picoseconds. After the timing stages, the four encoded pulses are made co-linear using a *multiplexer* arrangement. The  $1\omega S$  and  $1\omega P$  pulses are spatially overlapped using a polarizing beamsplitter (PBS). These two pulses are then spatially overlapped with the  $2\omega S$  pulse via a  $1\omega/2\omega$  dichroic beamsplitter (DBS). The final optic in the system for recombining is a non-polarizing beam splitter (BS) which enables the  $2\omega P$  pulse to overlap with the other pulses. The co-linear, temporally separated pulses are directed transversely, across the interaction of an intense laser pulse with a plasma, as an optical probe. The transmitted probe light is then directed to the *demultiplexer*, external to the vacuum chamber, where the co-linear probe pulses are split into four spatially separate channels. Here the demultiplexer consists of a dichroic beamsplitter and a pair of polarizing beamsplitters which enable the pulses to be split by wavelength and then by polarization, spatially separating the four individual pulses. The initial design of the imaging system consists of a Normarski-type interferometer [27] by passing each pulse through a Wollaston prism and a polarizer to produce an interference pattern [28]. Each of the channels is then imaged into a separate Andor Neo sCMOS camera. The use of interferometry is intended to

give a direct time resolved measurement of the evolving plasma electron density [29].

### 3. Experimental set up for use on high intensity laser–plasma interactions

The new optical probing technique was first tested in an intense laser–plasma interaction experiment. The multi-channel optical probe enables direct measurement of the propagation of a relativistically intense laser pulse in a high density sub-critical [30] plasma medium during a single interaction. The experiment was performed at the Rutherford Appleton Laboratory, Oxfordshire, UK, using the Vulcan Nd:Glass laser system in a dual short pulse beam configuration. The probe beam was picked off from a larger 20 cm diameter beam with a total energy of  $\approx 30$  J and a pulse duration of  $\approx 1$  ps. The probe beam was 2.54 cm in diameter with 480 mJ total energy.

The intense laser plasma interaction was driven by a 1054 nm laser with 150 J pulse energy and 20 ps duration at full width at half maximum (FWHM). The laser was focused to  $\approx 5.6 \mu\text{m}$  (FWHM) using an F/3 off-axis parabola, reaching a peak intensity of  $\approx 1 \times 10^{18} \text{ W/cm}^2$ . The laser was focused to the centre of a helium gas jet target, which was operated at pressures of up to 100 bar, reaching electron densities of up to  $1 \times 10^{20} \text{ cm}^{-3}$  ( $0.1 n_c$  [30]).

The optical probe was timed relative to this high intensity laser pulse using a streak camera. Although the streak camera could reach sub-2 ps temporal resolutions, the timing resolution between the optical probe and the high intensity pulse was found to be  $\approx \pm 10$  ps. This was due to jitter in the electrical signal used to trigger the streak camera. The time delay for each pulse was adjusted using a time delay slide which had 2 ns (60 cm) maximum range of motion in a double pass configuration. A magnescale encoder was used with a position accuracy of  $\approx 30$  fs ( $\approx 10 \mu\text{m}$ ). Initially all four optical probe pulses were overlapped in time with the high intensity pulse and then moved in time to provide measurements at defined points in the interaction. As shown in Fig. 2, a combination of transmissive and reflective optics were used, after the time delay system, to achieve spatial overlap between the four pulses. This process resulted in significant energy losses in some of the channels. The transmission through the multiplexer was calculated to be  $0.125E_t$  ( $1\omega\text{S}$ ),  $0.25E_t$  ( $1\omega\text{P}$ ),  $0.06E_t$  ( $2\omega\text{S}$ ), and  $0.06E_t$  ( $2\omega\text{P}$ ), where  $E_t$  is total input laser energy.

After the optical probe passed through the plasma and the individual pulses spatially separated in the *demultiplexer* system, the remaining sections of the optical probe were set up to act as a Normarski-type interferometer for each of the pulses. Although interferometry was tested and demonstrated to work during the experiment, the reduction in signal caused by the introduction of a polarizer and Wollaston prism was found to reduce the signal-to-noise to an unacceptable level during high power laser shots due to the production of self-emission [31]. The data presented in the following sections is therefore limited to shadowgraphy measurements only. The field of view of the optical probe imaging system was  $\approx 0.6 \text{ mm} \times 0.5 \text{ mm}$  with a resolution of  $\approx 7 \mu\text{m}$  at  $1\omega$  and  $\approx 3.5 \mu\text{m}$  at  $2\omega$ , in both dimensions, and magnification of  $\approx 29$ , for each of the channels.

### 4. Initial experimental results

Figures 3(a)–3(d) shows example measurements of the interaction of the intense laser pulse with a helium gas target at a gas pressure of  $P = 99.7, 98.1, 95.1$  and  $41.1$  bar respectively. From left to right in Fig. 3, each of the separate output channels of the probe are shown for fixed timings relative to the peak of the laser of  $t = 0, 12, 167$  and  $217$  ps, respectively. In these images the temporal evolution of a laser-driven plasma channel is clearly observed. The formation of such a channel is expected around the focal region due to the time-averaged ponderomotive force [32, 33], which acts to accelerate electrons away from regions of locally high intensity [18, 32, 34]. This depletion of electrons from the focal region results in an intensity dependent change in the refractive index [35]. For the approximately Gaussian focal spot distribution used in this experiment, the wings of the laser spatial-intensity profile propagate faster in the plasma than the intense center due to the higher electron density at edges of the



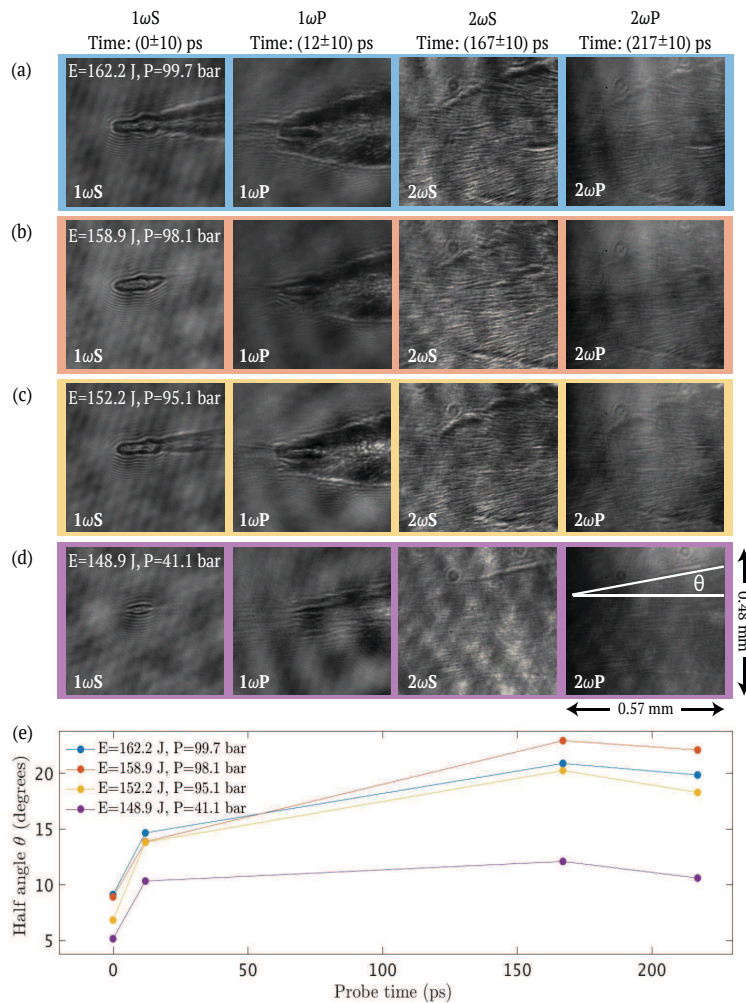


Fig. 3. Shadowgraphy measurements of each probe output channel from the experiment for (a)  $E = 162.2$  J,  $P = 99.7$  bar (b)  $E = 158.9$  J,  $P = 98.1$  bar (c)  $E = 152.2$  J,  $P = 95.1$  bar, and (d)  $E = 148.9$  J,  $P = 41.1$  bar. (e) Averaged half-angle ( $\theta$ ) divergence of the plasma channel wall evolving at 0, 12, 167 and 217 ps measured directly from the sets of images(a)–(d).

channel, resulting in a rapid self-focusing of the beam [7]. The peak laser intensity in this experiment is only slightly above the  $1.24 \times 10^{18}$  W/cm<sup>2</sup> relativistic threshold for the  $1.054 \mu\text{m}$  wavelength used here. In this regard, the plasma electron Lorentz factor is close to unity and so we expect ponderomotive self-focusing effects to dominate at early times. However, given sufficient ponderomotive self-focusing, relativistic effects could play a role near the peak of the pulse [7].

The most salient point to be taken from these measurements is the observed variability in the channel evolution, despite only small fluctuations in the laser and gas target parameters. Across the three examples of repeated laser shots Fig. 3(a)–3(c) the average gas pressure is  $98 \text{ bar} \pm 2 \text{ bar}$  ( $\pm 2\%$ ) and the average laser energy is  $158 \text{ J} \pm 5 \text{ J}$  ( $\pm 3\%$ ). In this range we observe the early evolution of the channel to change substantially. While in all cases there is a small region of plasma which forms at early times and then rapidly evolves into a full channel within 12 ps, in Fig. 3(a) and 3(c) we observe an earlier onset of the full channel. This variation in the channel

growth does not appear correlated with higher laser energy and plasma density alone, as in Fig. 3(c) both of these parameters are lower than in 3(b) where the early onset of the channel is not observed in the  $1\omega S$  measurements. This earlier onset of the channel formation will induce self-focusing, and at these densities beam collapse [33]. In the  $1\omega P$  measurements, a larger degree of filamentation is clearly observed for Fig. 3(a) and 3(c) where the channel formation occurred earliest. This early time channel evolution induced by small random variations in the laser - such as an additional prepulse - or plasma parameters is a quintessential example of the utility that the multi-channel optical probe can provide. In a standard single channel optical probe arrangement the temporal dynamics are extracted over consecutive repeated laser shots, where it is impossible to differentiate the evolution of the plasma dynamics from random fluctuations in the initial conditions. Such an insight into the evolving stability of channel formation would be of particular interest for the fast ignitor concept in inertial confinement fusion [36].

The measurements for the later channels show a stagnation of the channel evolution for  $t \geq 150$  ps, long after the laser pulse has passed. The  $2\omega S$  and  $2\omega P$  channels both suffer poor signal-to-noise ratio due to pick up of the plasma self-emission. The stagnation in the evolution of the channel is clearly observed in Fig. 3(e) where at early time the channel half angle is shown to grow rapidly then saturate on time scales longer than the laser pulse duration. The half angle  $\theta$  is calculated as defined in Fig. 3(d), overlaid on the the  $2\omega P$  channel. The initial half-angle of the channel shown in Fig. 3(a)–3(c) is approximately  $10^\circ$ , which is expected for the F/3 focusing geometry used in this experiment and suggests that limited ponderomotive self-focusing has occurred early in the interaction. Later in the interaction for  $t \geq 12$  ps the angle of the channel has increased up to near  $15^\circ$  which is approaching an F/2 focusing geometry, induced by self-focusing of the laser pulse. The measurements at late time show an even steeper profile which is approaching an F/1 focusing geometry, which has then saturated by the final time step. In addition to the images shown in Fig. 3(a)–3(c), this measurement is also made, for comparison, for  $P = 41.1$  bar and  $E = 148.9$  J in Fig. 3(d) and the evolution is quite different. At early times breakdown of the background is observed but the full channel has not yet formed. For  $t \geq 12$  ps a channel is present with a half-angle which approaches the initial F/3 geometry and remains approximately constant for the succeeding time steps.

These measurements provide insight into the evolving picosecond-scale dynamics of laser-pulse propagation in underdense plasma and their sensitivity to fluctuations in initial plasma conditions and laser input parameters. This data highlights the importance of reproducible conditions to ensure reliability, especially when measurements are reconstructed from a series of consecutive shots.

## 5. Summary and outlook

A multi-channel optical probe capable of both 2D spatial resolution and picosecond-scale temporal resolution of a single laser pulse–plasma interaction has been developed. Example experimental results demonstrate the utility of this approach, where random fluctuations in the laser and plasma parameters on the order of a few percent have been observed to modify the plasma channel evolution substantially and therefore the laser–pulse propagation dynamics. This highlights the need to employ single-shot time-resolved measurements in order to clearly deconvolve random fluctuations in experiment parameters from changes in the dynamics. Equivalent measurements cannot be made using a conventional single time frame optical probe approach. Future development of this approach will open up single-shot electron density evolution measurements via time-resolved interferometry and higher temporal resolution by modifying the system to be appropriate for femtosecond-scale laser pulses. Achieving femtosecond-scale temporal resolution would involve careful consideration of dispersive effects due to the increased bandwidth but would be possible via increased use of thin pellicle beam splitters and reflective waveplates. Due to the reduced energy, gains in throughput efficiency would also be required principally by modifying

the layout of the multiplexer system to remove the broadband beam splitter which is responsible for significant energy losses. The development of this system supports the growing capacity in the field to make controlled and precise time-resolved measurements of intense laser-plasma interactions. This will enable new insight into the underpinning physics which drive, for example, laser-driven radiation sources and which previously could not be measured experimentally during a single interaction. The novel concept presented here also has the potential to be extended and adapted for cross-disciplinary research interests which could benefit from temporally resolving ultrafast processes and particularly in cases where the underlying dynamics appear stochastic.

## Funding

Engineering and Physical Sciences Research Council (EPSRC) (EP/R006202/1, EP/M018091/1, EP/J003832/1). Data associated with research published in this paper can be accessed at: <https://doi.org/10.15129/aed278e4-ba1e-4653-880c-72a58e4b7803>

## Acknowledgments

The authors acknowledge the expertise of the Central Laser Facility staff.

## Disclosures

The authors declare that there are no conflicts of interest related to this article.

## References

1. M. Tabak, J. Hammer, M. E. Glinsky, W. L. Kruer, S. C. Wilks, J. Woodworth, E. M. Campbell, and M. D. Perry, "Ignition and high gain with ultrapowerful lasers," *Phys. Plasmas*, **1**, 1626–1634 (1994).
2. S. Cipiccia, M. R. Islam, B. Ersfeld, R. P. Shanks, E. Brunetti, G. Vieux, X. Yang, R. C. Issac, S. M. Wiggins, G. H. Welsh, M. Anania, D. Maneuski, R. Montgomery, G. Smith, M. Hoek, D. J. Hamilton, N. R. C. Lemos, D. Symes, P. P. Rajeev, V. O. Shea, J. M. Dias, and D. A. Jaroszynski, "Gamma-rays from harmonically resonant betatron oscillations in a plasma wake," *Nat. Phys.* **7**, 867–871 (2011).
3. A. J. Gonsalves, K. Nakamura, C. Lin, D. Panasenko, S. Shiraishi, T. Sokollik, C. Benedetti, C. B. Schroeder, C. G. R. Geddes, J. Van Tilborg, J. Osterhoff, E. Esarey, C. Toth, and W. P. Leemans, "Tunable laser plasma accelerator based on longitudinal density tailoring," *Nat. Phys.* **7**, 862–866 (2011).
4. A. Higginson, R. J. Gray, M. King, S. D. R. Williamson, N. H. M. Butler, R. Wilson, R. Capdessus, C. Armstrong, J. S. Green, S. J. Hawkes, P. Martin, W. Q. Wei, S. R. Mirfayzi, X. H. Yuan, S. Kar, M. Borghesi, R. J. Clarke, D. Neely, and P. McKenna, "Near-100 MeV protons via a laser-driven transparency-enhanced hybrid acceleration scheme," *Nat. Commun.* **9**, 724 (2018).
5. B. Gonzalez-Izquierdo, R. J. Gray, M. King, R. J. Dance, R. Wilson, J. McCreadie, N. M. H. Butler, R. Capdessus, S. Hawkes, J. S. Green, M. Borghesi, D. Neely, and P. McKenna, "Optically controlled dense current structures driven by relativistic plasma aperture-induced diffraction," *Nat. Phys.* **12**, 505–512 (2016).
6. R. J. Gray, D. C. Carroll, X. H. Yuan, C. M. Brenner, M. Burza, M. Coury, K. L. Lancaster, X. X. Lin, Y. T. Li, D. Neely, M. N. Quinn, O. Tresca, C.-G. Wahlström, and P. McKenna, "Laser pulse propagation and enhanced energy coupling to fast electrons in dense plasma gradients," *New J. Phys.* **16**, 113075 (2014).
7. M. R. Siegrist, "Self-focusing in a plasma due to ponderomotive forces and relativistic effects," *Opt. Commun.* **16**, 402–407 (1976).
8. J. Vieira, J. T. Mendonça, and F. Quéré, "Optical control of the topology of laser-plasma accelerators," *Phys. Rev. Lett.* **121**, 054801 (2018).
9. M. Borghesi, A. Schiavi, D. H. Campbell, M. G. Haines, O. Willi, A. J. MacKinnon, L. A. Gizzi, M. Galimberti, R. J. Clarke, and H. Ruhl, "Proton imaging: a diagnostic for inertial confinement fusion/fast ignitor studies," *Plasma Phys. Control. Fusion* **43**, 267–276 (2001).
10. L. Willingale, P. M. Nilson, A. G. R. Thomas, J. Cobble, R. S. Craxton, A. Maksimchuk, P. A. Norreys, T. C. Sangster, R. H. H. Scott, C. Stoeckl, C. Züllick, and K. Krushelnick, "High-power, kilojoule class laser channeling in millimeter-scale underdense plasma," *Phys. Rev. Lett.* **106**, 105002 (2011).
11. D. J. Bradley, B. Liddy, and W. E. Sleat, "Direct linear measurement of ultrashort light pulses with a picosecond streak camera," *Opt. Commun.* **2**, 391–395 (1971).
12. S. Jackel, B. Perry, and M. Lubin, "Dynamics of laser-produced plasmas through time-resolved observations of  $2\omega_0$  and  $\frac{3}{2}\omega_0$  harmonic light emissions," *Phys. Rev. Lett.* **37**, 95–98 (1976).
13. L. Volpe, D. Batani, B. Vauzour, P. Nicolai, J. J. Santos, C. Regan, A. Morace, F. Dorchies, C. Fourment, S. Hulin, F. Perez, S. Baton, K. Lancaster, M. Galimberti, R. Heathcote, M. Tolley, C. Spindloe, P. Koester, L. Labate, L.



- A. Gizzi, C. Benedetti, A. Scattoni, M. Richetta, J. Pasley, F. Beg, S. Chawla, D. P. Higginson, and A. G. MacPhee, "Proton radiography of laser-driven imploding target in cylindrical geometry," *Phys. Plasmas* **18**, 012704 (2011).
14. A. J. Mackinnon, P. K. Patel, R. P. Town, M. J. Edwards, T. Phillips, S. C. Lerner, D. W. Price, D. Hicks, M. H. Key, S. Hatchett, S. C. Wilks, M. Borghesi, L. Romagnani, S. Kar, T. Toncian, G. Pretzier, O. Willi, M. Koenig, E. Martinolli, S. Lepape, A. Benuzzi-Mounaix, P. Audebert, J. C. Gauthier, J. King, R. Snavely, R. R. Freeman, and T. Boehlly, "Proton radiography as an electromagnetic field and density perturbation diagnostic," *Rev. Sci. Instrum.* **75**, 3531–3536 (2004).
15. H. Shiraga, M. Nakasuji, M. Heya, and N. Miyanaga, "Two-dimensional sampling-image x-ray streak camera for ultrafast imaging of inertial confinement fusion plasma," *Rev. Sci. Instrum.* **70**, 620–623 (1999).
16. J. S. Green, C. D. Murphy, N. Booth, R. J. Dance, R. J. Gray, D. A. MacLellan, P. McKenna, D. Rusby, and L. Wilson, "Single shot, temporally and spatially resolved measurements of fast electron dynamics using a chirped optical probe," *J. Instrum.* **9**, P03003 (2014).
17. P. Antici, S. N. Chen, L. Gremillet, T. Grismayer, P. Mora, P. Audebert, and J. Fuchs, "Time and space resolved interferometry for laser-generated fast electron measurements," *Rev. Sci. Instrum.* **81**, 113302 (2010).
18. Z. Najmudin, K. Krushelnick, M. Tatarakis, E. L. Clarke, C. N. Danson, V. Malka, D. Neely, M. I. K. Santala, and A. E. Dangor, "The effect of high intensity laser propagation instabilities on channel formation in underdense plasmas," *Phys. Plasmas* **10**, 438–442 (2003).
19. J. Liang and L. V. Wang, "Single-shot ultrafast optical imaging," *Optica* **5**, 1113–1127 (2018).
20. Z. Li, H. Tsai, X. Zhang, C. Pao, Y. Change, R. Zgadzaj, X. Wang, V. Khudik, G. Shvets, and M. C. Downer, "Single-shot visualization of evolving plasma wakefields," *AIP Conf. Proc.* **1117**, 040010 (2016).
21. S. P. D. Mangles, A. G. R. Thomas, O. Lundh, F. Lindau, M. C. Kaluza, A. Persson, C.-G. Wahlström, K. Krushelnick, and Z. Najmudin, "On the stability of laser wakefield electron accelerators in the monoenergetic regime," *Phys. Plasmas* **14**, 056702 (2007).
22. S. P. D. Mangles, C. D. Murphy, Z. Najmudin, A. G. R. Thomas, J. L. Collier, A. E. Dangor, E. J. Langley, W. B. Mori, P. A. Norreys, F. Z. Tsung, R. Viskup, B. R. Walton, and K. Krushelnick, "Monoenergetic beams of relativistic electrons from intense laser-plasma interactions," *Nature* **431**, 535–538 (2004).
23. M. C. Kaluza, M. I. K. Santala, J. Schreiber, G. D. Tsakiris, and K. J. White, "Time-sequence imaging of relativistic laser-plasma interactions using a novel two-color probe," *Appl. Phys. B* **92**, 475–479 (2008).
24. D. Grossmann, M. Reininghaus, C. Kalupka, M. Kumkar, and R. Poprawe, "Transverse pump-probe microscopy of moving breakdown, filamentation and self-organized absorption in alkali aluminosilicate glass using ultrashort pulse laser," *Opt. Express* **24**, 23221 (2016).
25. P. R. Poulin and K. A. Nelson, "Irreversible organic crystalline chemistry monitored in real time," *Science* **313**, 1756–1760 (2006).
26. K. Ward, "A short history of telecommunications transmission in the UK," *J. Commun. Net.* **5**, 30–41 (2006).
27. M. Börner, J. Fils, A. Frank, A. Blažević, T. Hessling, A. Pelka, G. Schaumann, A. Schökel, D. Schumacher, M. M. Basko, J. Maruhn, A. Tauschwitz, and M. Roth, "Development of a Nomarski-type multi-frame interferometer as a time and space resolving diagnostic for the free electron density of laser-generated plasma," *Rev. Sci. Instrum.* **83**, 043501 (2012).
28. R. Benattar, C. Popovics, and R. Sigel, "Polarized light interferometer for laser fusion studies," *Rev. Sci. Instrum.* **50**, 1583–1586 (1979).
29. L. B. Da Silva, T. W. Barbee, Jr., R. Cauble, P. Celliers, D. Ciarlo, S. Libby, R. A. London, D. Matthews, S. Mrowka, J. C. Moreno, D. Röss, J. E. Trebes, A. S. Wan, and F. Weber, "Electron density measurements of high density plasmas using soft x-ray laser interferometry," *Phys. Rev. Lett.* **74**, 3991–3994 (1995).
30. T. J. M. Boyd and J. J. Sanderson, *The Physics of Plasma* (Cambridge University, 2003).
31. S. D. Baton, H. A. Baldis, T. Jalinou, and C. Labaune, "Fine-scale spatial and temporal structures of second harmonic emission from an underdense plasma," *Europhys. Lett.* **23**, 191–196 (1993).
32. E. Esarey, C. B. Schroeder, B. A. Shadwick, J. S. Wurtele, and W. P. Leemans, "Nonlinear theory of nonparaxial laser pulse propagation in plasma channels," *Phys. Rev. Lett.* **84**, 3081–3084 (2000).
33. R. Fedosejevs, X. F. Wang, and G. D. Tsakiris, "Onset of relativistic self-focusing in high density gas jet targets," *Phys. Rev. E* **56**, 4615–4639 (1997).
34. G. A. Askaryan, "Waveguide properties of a tubular light beam," *Zh. Eksp. Teor. Fiz.* **28**, 732–733 (1969).
35. D. Umstadter, "Relativistic laser-plasma interactions," *J. Phys. D: Appl. Phys.* **36**, 151–165 (2003).
36. S. Ivancic, D. Haberberger, H. Habara, T. Iwakaki, K. S. Anderson, R. S. Craxton, D. H. Froula, D. D. Meyerhofer, C. Stoeckl, K. A. Tanaka, and W. Theobald, "Channeling of multikilojoule high-intensity laser beams in an inhomogeneous plasma," *Phys. Rev. E* **91**, 051101 (2015).